

# **On-line Optimization-Based Simulators for Fractured and Non-fractured Reservoirs**

***DE-FC26-01BC15313***

*Principal Investigator: Milind D. Deo  
Department of Chemical and Fuels Engineering  
University of Utah  
Salt Lake City, Utah 84112*

**An Interim Report on**

## **Generating Representative Fault/Fracture Systems for Reservoir Simulation**

**Prepared by**

*Craig B. Forster and Jeffrey T. Dunn*

Disclaimer:

This report was prepared an account of work sponsored by an agency of the United States Government. Neither the United States Government nor any agency thereof, nor any of their employees, makes any warranty, express or implied, or assumes any legal responsibility for the accuracy, completeness, or usefulness of any information, apparatus, product or process disclosed, or represents that its use would not infringe privately owned rights. Reference herein to any specific commercial product, process, or service by trade name, trademark, manufacturer, or otherwise does not necessarily constitute or imply its endorsement, recommendation, or favoring by the United States Government or any agency thereof. The views and opinions of authors expressed herein do not necessarily state or reflect those of the United States Government or any agency thereof.

## **1.0 Introduction**

Faults and fractures can play a key role in controlling fluid flow through hydrocarbon reservoirs. Unfortunately, the small thickness (typically less than 1 mm for fractures, and less than 10 m for faults) and the often sub-vertical orientation of these semi-planar geologic features make them difficult, to impossible, to locate in the subsurface; except as they might be encountered in drill core or expressed in borehole geophysical logs. Interpolating the 3-dimensional geometries of fault/fracture networks between wells, even when accompanied by ground surface geophysical surveys, requires interwell information that cannot be obtained from the subsurface. As a consequence, we use observations made in outcropping exposures of faulted and fractured rock to guide the process of generating representative fault/fracture systems that can be plausibly incorporated into reservoir simulators.

This report focuses on the results of our own studies aimed at assessing the role of faults and fractures in controlling fluid flow through Navajo Sandstone exposed in Southern Utah (e.g., Shipton et al., 2002; Dunn, 2004). We, and others, have completed similar outcrop-based studies in faults found in sandstone and other rock types (e.g., Aydin, 1978; Forster and Evans, 1991; Antonellini and Aydin, 1994, 1995; Caine et al., 1996; Matthai et al., 1998; Forster et al., 1998; Caine and Forster, 1999; Davis, 1999; Taylor et al., 1999; Maerten et al., 2001; Jourde et al., 2002). The Big Hole Fault (Shipton et al., 2002) and Teasdale Fault Zone (Dunn, 2004) have received much of our attention over the past 5 years because they are well exposed at the surface and provide a wide spectrum of fault type within the relatively uniform sandstone host rock. Fault-

affected sandstone at the Big Hole Fault has suffered reduced permeability as a consequence of faulting through the formation of deformation bands (thin, planar fracture-like features comprising finely ground sandstone grains). Both high-permeability fractures and low-permeability deformation bands are associated with the Teasdale Fault Zone. The following sections outline how we use the outcrop data to generate the input to fluid flow simulations designed to explore the way high, and low, permeability fault-related features control fluid flow through high-permeability sandstone reservoir rock. Lessons learned at both the Big Hole Fault and Teasdale Fault Zone are illustrated using the results of our work at the Teasdale Fault Zone.

## **2.0 Approach**

Our approach to generating fault/fracture input to reservoir simulators is grounded in well-established methods of mapping fault-related structures (fractures, fault gouge, deformation bands, etc.) in outcrop. The canyon-mesa topography of Southern Utah is ideal for providing access to 3-dimensional views of the vertical and lateral extent of features that control fluid flow but cannot be imaged in the subsurface with geophysical methods. Field activities include: (1) detailed measurements of the frequency, orientation, length and character of small, fault-related features along vertical and horizontal transects ranging from 10s to 100s of meters in length, and (2) field and aerial photo based surveys of the larger fault networks with individual, kilometer-scale fault lengths and fault widths on the order of 1s to 10s of meters. The results of mapping across scales ranging from millimeters to several kilometers provide the geometrical information needed as input to reservoir simulators. As the fault-related features are

mapped in the field, their character is identified so that appropriate estimates of fluid flow properties can be assigned to individual faults within each fault network. We use simple averaging methods to estimate effective permeability tensors and porosity values based on the number and character of fault-related features found within, and near, kilometer-scale faults. The 40 km long Teasdale Fault Zone (Figure 1) provides a good illustration of our approach because it contains both high-permeability, fracture-dominated features and low-permeability deformation band dominated features within a major fault zone that exhibits major variations in character and geometry along the fault.

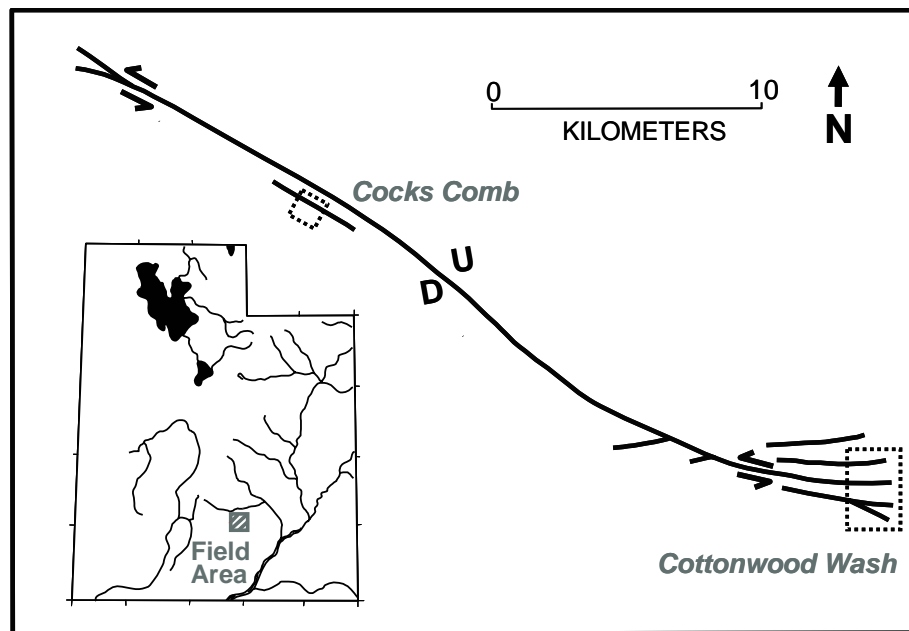


**Figure 1.** Location and map view of the 40 km long, NW-SE trending Teasdale Fault Zone in Southern Utah. Two principal study areas are indicated; the Cocks Comb and Cottonwood Wash (mapping results shown in detail in Figure 2). Sense of motion is

reverse slip at the middle of the fault (shown with **D** (down) and **U** (up)) and strike slip at each end (shown with arrows). After Dunn (2004).

### **3.0 Data Synthesis**

#### ***Fault Network Scale***

The results of km-scale field mapping and aerial photo surveys are synthesized to create detailed maps of the fault networks that comprise the Teasdale Fault Zone (Figure 2). Fault networks and fault-affected rock were mapped at two key locations; at the Cocks Comb and at Cottonwood Wash (Figure 1). At the mid-fault, Cocks Comb, location (Figure 2a) the Teasdale Fault Zone experienced reverse slip with the resulting fault networks being well preserved in the outcrops of the upthrown (**U**) fault block of Navajo Sandstone. The strike slip motion experienced at the eastern, Cottonwood Wash, end of the Teasdale Fault Zone (Figure 2b) yields a much broader fault zone in exposed in Navajo Sandstone with greater spacing between individual faults of the fault network. Both locations contain faults filled with fractures and faults filled with deformation bands. Individual faults filled with deformation bands are usually aligned with the trace of the Teasdale Fault Zone. Faults filled with fractures typically cut across the fault zone. The widths of individual faults range from 1 to 10 meters.

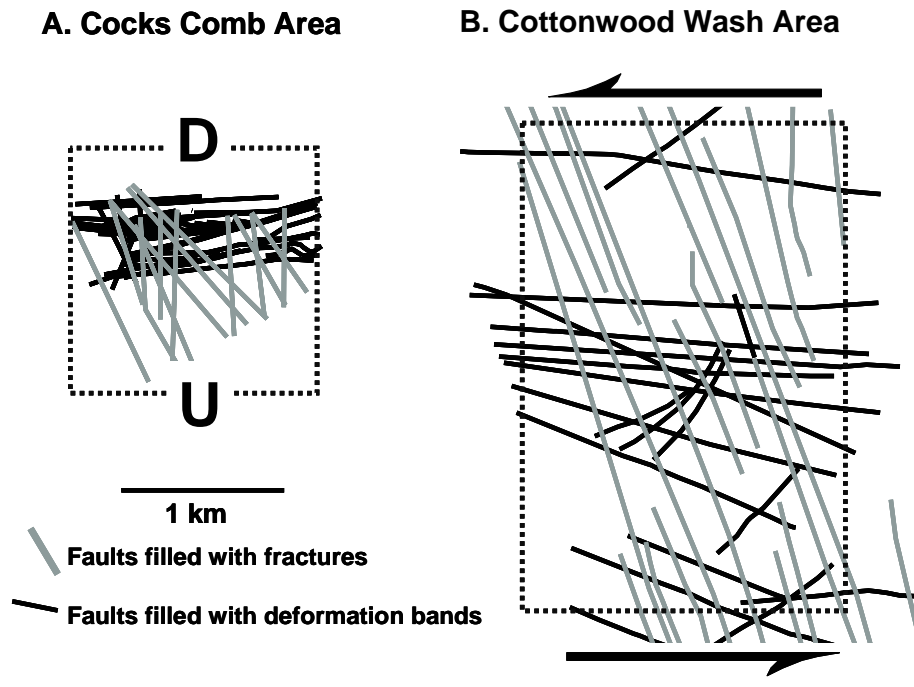


**Figure 2.** Plan view distribution of fracture-filled and deformation band filled faults associated with two locations along the Teasdale Fault Zone (Figure 1): (a) Cocks Comb area (reverse sense of motion shown with **D** (down) and **U** (up)), and (b) Cottonwood Wash area (strike slip sense of motion shown with arrows). The main trace of the Teasdale fault runs from left to right across each study area. The dotted rectangles show the outer boundary of the finite element grids developed to capture the properties of the fault systems in a fluid flow simulator. After Dunn (2004).

The fault networks shown in Figure 2 are used to create gridded, 3-dimensional finite element flow simulation domains by representing each individual fault with a series of prismatic, 3-D elements (Figure 3). The faults are assumed vertical in creating the simulation grids of Figure 3. Although this approach provides useful insight regarding the impact of the faults on fluid flow, we will ultimately represent the individual faults as

groups of planar elements embedded in a field of 3-D prismatic elements. Field mapping indicates that smaller, fault-related features than those shown in Figure 2, and captured in the grids of Figure 3, are limited in number and extent. Thus, those features need not be explicitly represented in the simulation grid. The way such features might affect fluid flow properties of the intervening rock, however, can be represented by adjusting the properties of the intervening sandstone host rock.

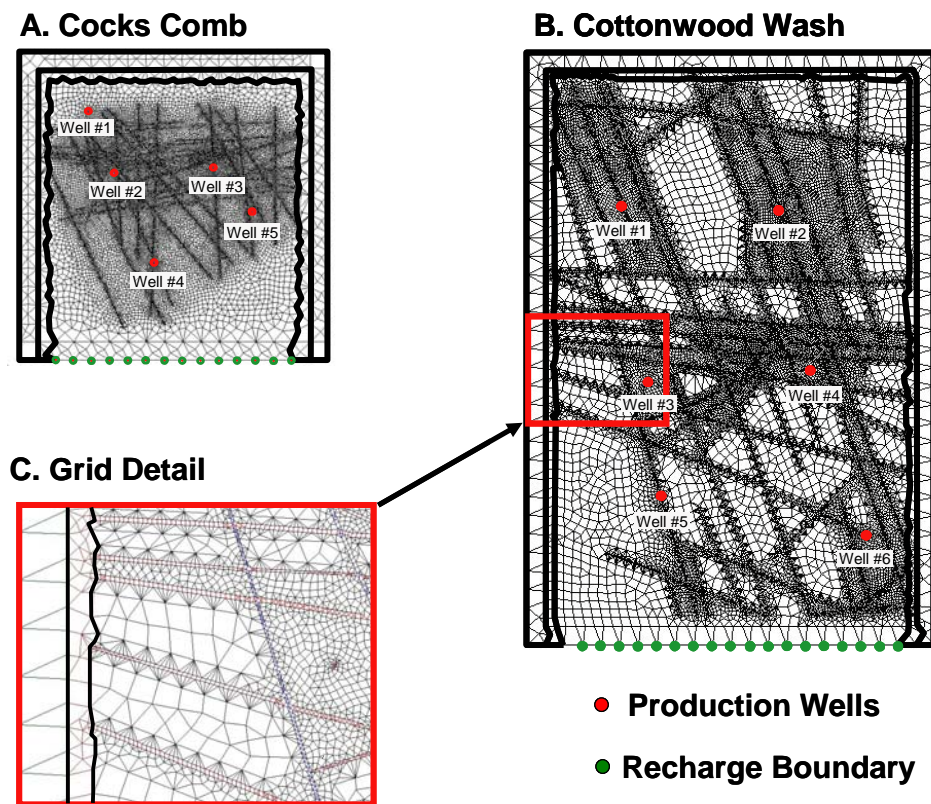


**Figure 3.** Plan view of finite element simulator domains constructed to capture the individual fault network geometries shown in Figure 2: (a) Cocks Comb model domain, (b) Cottonwood Wash model domain, and (c) detail of Cottonwood Wash grid. All boundaries are impermeable, except the recharge boundaries located at the page-bottom side of each domain. After Dunn (2004).

### ***Individual Fault Scale***

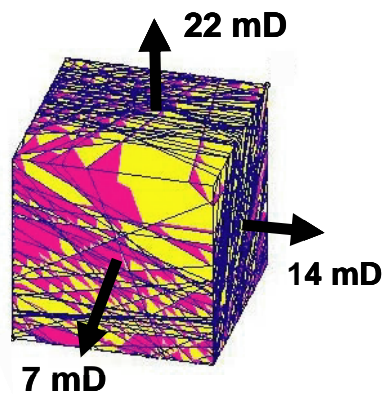
Data collected by mapping features encountered in relatively short (1s to 10s of meters) vertical and horizontal transects are used to estimate the fluid flow properties of the grid elements used to represent individual fault zones. This method yields a one-dimensional representation of the location and intensity of fractures, small faults and deformation bands found within and between individual larger faults. Transect data include type of feature, position, orientation, apparent thickness or aperture, geometry and relative age relationships between footwall and hanging wall. Where groups of closely-spaced, amalgamated deformation bands were mapped, the cumulative thickness of deformation band material per meter was noted.

The detailed data collected in the transect mapping were compiled so that synthetic network models of fractures or deformation bands could be constructed within 2 m on-a-side cubes of sandstone (Figure 4). Deformation band network models (Figure 4a) are constructed using Golder Associates' FRACWORKS® 95 computer program; a component of the FRACMAN® software package used to generate three-dimensional realizations of fracture networks. Effective permeability in directions parallel to each side of the block are estimated by computing the thickness-weighted harmonic mean of the sandstone host rock (500 mD) and deformation bands (1 mD and 1 mm thickness) sampled along digital transects cut through the block (Figure 4a). The relatively high intensity of deformation bands, oriented in various directions, leads to almost isotropic permeability of about 15 mD (7 mD perpendicular to the fault, 22 mD parallel to fault dip

and 14 mD parallel to the trace of the fault) within deformation band dominated faults; for the conditions specified (Figure 4a).

A continuum approach is used to estimate effective permeability values in fracture networks (Oda, 1985). Joints are typically near-vertical and approximately parallel to one another. Field observations indicate that zones of through-going joints are often composed of 40 to 50 joints over a span of 2 to 3 m (Figure 4b). In this example, permeability tensors are calculated for joint zones assuming 25 joints per meter and a fixed aperture of 100  $\mu\text{m}$  intersecting a 2-cubic meter volume. A sandstone permeability of 500 mD and a deformation band zone permeability of 20 mD are also used. Calculated values of effective permeability for the 500 mD sandstone are 379 mD in the direction perpendicular ( $k_{\perp}$ ) to the fault, 3631 mD in the direction parallel to the strike ( $k_{//S}$ ) of the fault, and 2508 md in the direction parallel to the dip ( $k_{//D}$ ) of the fault. The preferred orientation of joints found in the faults leads to this strong anisotropy with maximum permeability within the fault plane and minimum permeability normal to the fault. Computed permeability values for jointed deformation band zones with 25 joints per meter intersecting 20 md rock are  $k_{\perp} = 23$  md,  $k_{//S} = 2547$  md and  $k_{//D} = 2508$  md.

## A. Deformation Bands



## B. Fractures

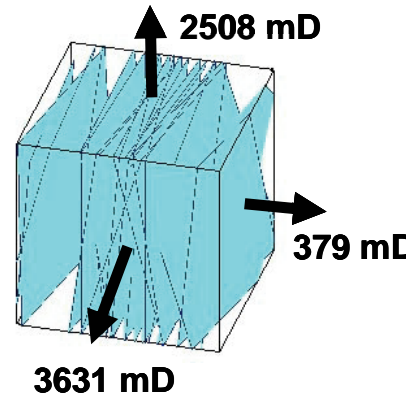


**Figure 4.** Synthetic network models in 2 m on-a-side cubes of sandstone constructed as a foundation for computing effective permeability in three principal coordinate directions (parallel to the fault trace [left to right], normal to the fault plane [in and out of the page] and parallel to fault dip [up and down]): (a) deformation band network with 1 mm thick deformation bands of 1 mD permeability in 500 mD sandstone, and (b) fracture network with 100  $\mu$ m aperture fractures in 500 mD sandstone. After Dunn (2004).

The finite element grids shown in Figure 3 are populated with fault-related parameter values that reflect the average permeability and porosity values computed at the 2-m block scale (Figure 4). The large anisotropy of the fracture-filled faults suggests that these features can be plausibly represented at lower computational cost by replacing the 3-D prismatic elements with 2-D planar fracture elements embedded within a domain of much larger, 3-D prismatic elements that represents the sandstone host rock.

## References

- Antonellini, M., and A. Aydin, 1994, Effect of faulting on fluid flow in porous sandstones: petrophysical properties: AAPG Bulletin, v. 78, p. 355-377.
- Antonellini, M., and A. Aydin, 1995, Effect of faulting on fluid flow in porous sandstones: geometry and spatial distribution: AAPG Bulletin, v. 79, p. 642-671.
- Aydin, A., 1978, Small faults formed as deformation bands in sandstones: Pure and Applied Geophysics, v. 116, p. 913-930.
- Caine, J. S., J.P. Evans, and C.B. Forster, 1996, Fault zone architecture and permeability structure: Geology, v. 24, p. 1025-1028.
- Caine, J.S., and C.B. Forster, 1999, Fault zone architecture and fluid flow, insights from field data and numerical modeling: faults and subsurface fluid flow in the shallow crust: Geophysical Monograph 113, American Geophysical Union, p. 101-127.
- Davis, G.H., 1999, Structural geology of the Colorado Plateau region of southern Utah, with special emphasis on deformation bands: Geological Society of America Special Paper 342. 157 p.
- Dunn, J.T., 2004, Variability of Reservoir Properties along the Teasdale Fault, Utah: Implications for Reservoir Production, M.S. Thesis, Dept. of Geology & Geophysics, University of Utah.
- Forster, C.B., and J.P. Evans, 1991, Hydrogeology of thrust faults and crystalline thrust sheets: results of combined field and modeling studies: Geophysical Research Letters, v. 18, p. 979-982.
- Forster, C.B., Nielson, D.L., and M. Deo, 1998, Characterization and simulation of an exhumed fractured petroleum reservoir, Final Report, U.S. Dept. of Energy, National Petroleum Technology Office, DOE/PC/91008-18.
- Jourde, H., E.A. Flodin, A. Aydin, L.J. Durlofsky, and X.-H. Wen, 2002, Computing permeability of fault zones in eolian sandstone from outcrop measurements: AAPG Bulletin, v. 86, p. 1187-1200.
- Maerten, L., Pollard, D.D., and Maerten, F., 2001, Digital mapping of three-dimensional structures of the Chimney Rock fault system, central Utah. Journal of Structural Geology, v. 23, p. 585-592.

- Matthai, S.K., A. Aydin, D. D. Pollard, and S. G. Roberts, 1998, Numerical simulation of departures from radial drawdown in a faulted sandstone reservoir with joints and deformation bands: in Jones, G., Q. J. Fisher, and R. J. Knipe, 1998, Faulting, fault sealing and fluid flow in hydrocarbon reservoirs: Geological Society, London, Special Publications 147, p. 157-191.
- Oda, M., 1985, Permeability tensor for rock masses: *Geotechnique* 35, no. 4, p. 483-495.
- Shipton, Z.K., Evans, J.P., Robeson, K., Forster, C.B. and S.H. Snelgrove, 2002, Structural heterogeneity and permeability in faulted eolian sandstone: implications for subsurface modelling of faults. *American Association of Petroleum Geologists Bulletin*, v. 86. p. 863-883.
- Taylor, W.L., Pollard D.D., and A. Aydin, 1999, Fluid flow in discrete joint sets: *Journal of Geophysical Research*, v. 104, no. B12, p. 28,983-29,006.